Rectangular Waveguide Output Unitraveling-Carrier Photodiode Module for High-Power Photonic Millimeter-Wave Generation in the F-Band

Hiroshi Ito, *Senior Member, IEEE*, Tsuyoshi Ito, *Member, IEEE*, Yoshifumi Muramoto, Tomofumi Furuta, and Tadao Ishibashi, *Senior Member, IEEE*

***Abstract*—A compact unitraveling-carrier photodiode (UTC-PD) module with a WR-8 rectangular waveguide output port for operation in the F-band (90–140 GHz) has been developed. A resonating matching circuit integrated with a UTC-PD and a microstrip-line-to-rectangular-waveguide transformer are designed to have high output powers with a wide bandwidth covering the F-band. The module size and configuration are equivalent to those of conventional optoelectronic devices, which enables the use of standard assembly technology. The fabricated module exhibits a record millimeter-wave output power of 17 mW at 120 GHz for a bias voltage of −3 V. The 3-dB bandwidth is as wide as 55 GHz, which fully covers the F-band. An optical input stress test at a photocurrent of 10 mA performed to confirm the long-term stability of the module showed that the dark current stays below 1 μA for more than 4000 hours.**

***Index Terms*—Impedance transformer, millimeter-wave generation, rectangular waveguide output module, semiconductor heterojunction, unitraveling-carrier photodiode.**

I. Introduction

PHOTONIC generation of millimeter (mm) and sub-mm wave signals is a promising technique because it provides several advantages, such as an extremely wide bandwidth afforded by the characteristics of optical components, and can use low-loss fibers for transmission of very-high-frequency signals. In addition, the use of a high-output-power opto-electronic (O/E) conversion device can eliminate the costly postamplification circuit and thus simplify the system configuration. The technology can be used for various applications, including fiber-radio wireless communications systems [1], high-speed measurement systems [2], mm-wave imaging systems [3], and a local signal supply for radio telescopes [4]. These systems require a photodiode that has high output power as well as superior high-frequency characteristics. The unitraveling-carrier photodiode (UTC-PD) [5] is one of the best solutions, because it provides a high 3-dB bandwidth ($f_{3\,\mathrm{dB}}$) and a high-saturation-output power simultaneously. To date, excellent performance—an $f_{3\,\mathrm{dB}}$ of 310 GHz [6] and an output power of over 20 mW at 100 GHz [7]—has been demonstrated. These features come from the unique operation mode of the UTC-PD, in which only electrons are the active carriers traveling through the junction depletion region [5]. For practical use, especially in the frequency range above 100 GHz, the device should be in a module with a rectangular waveguide (WG) output port, because the useful frequency range of the coaxial connector is limited to below ∼100 GHz. Although photodiode modules with a waveguide output port have been reported [8], [9], they are generally bulky and incompatible with the standard O/E device assembly technology. In addition, the obtained output power from those PD modules is limited to less than 0.2 mW at 110 GHz for a pin-PD [8] and 2 mW at 100 GHz for a UTC-PD [9]. Recently, we have developed a compact waveguide output UTC-PD module for operation in the W-band (75–110 GHz) [10]. This module exhibits a very high mm-wave output power of 11 mW at 100 GHz, which is about two orders of magnitude larger than that obtainable by a pin-PD module [8] at the same frequency. Despite these promising results, there still is a strong requirement [11] for developing photodiode modules operating at frequencies beyond the W-band, where the frequency range cannot be covered by coaxial connector technology.

In this paper, we develop a WR-8 waveguide output UTC-PD module for operation in the F-band (90–140 GHz). Its size and configuration are equivalent to those of conventional semiconductor O/E devices, so that it is compatible with standard assembly/testing equipment for O/E device modules. The module is designed to generate high output power in the F-band, and the output power characteristics as well as the stability for long-term operation are evaluated.

II. Design of Matching Circuit and Transformer

At frequencies above 100 GHz, it is important to implement methods for improving output power, because the influence of the CR time constant of the PD becomes significant in a conventional wide-band design. A resonating matching circuit is a promising technique to improve O/E conversion efficiency, which it achieves by compensating the imaginary part of the internal impedance in the UTC-PD at a designed frequency. The matching allows us to use a relatively large area (large junction capacitance) device to increase saturation photocurrent level and reduce self-heating of the PD. In particular, a short-stub matching circuit [7], [12] is a good solution for its simplicity, ease of integration with the UTC-PD, and limited number of optimizing parameters. Thus, the characteristics of

Manuscript received June 4, 2003; revised August 20, 2003.

H. Ito, T. Ito, Y. Muramoto, and T. Furuta are with NTT Photonics Laboratories, NTT Corporation, 243-0198 Kanagawa, Japan.

T. Ishibashi is with NTT Electronics Corporation, 194-0004 Tokyo, Japan.

Digital Object Identifier 10.1109/JLT.2003.821747

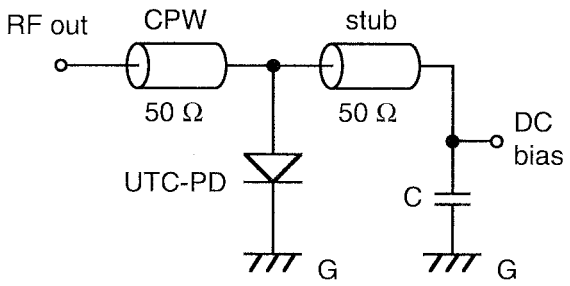

Fig. 1. Circuit diagram of a UTC-PD integrated with a short-stub matching circuit.

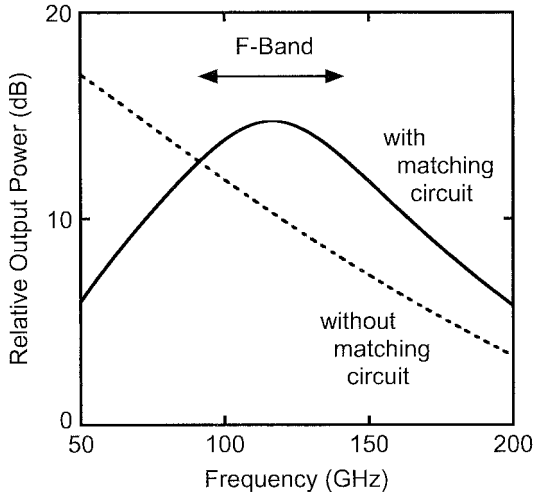

Fig. 2. Calculations of relative output power against frequency for a matching-circuit-integrated UTC-PD and a discrete UTC-PD.

the circuit diagramed in Fig. 1 were calculated based on an analytical model. The circuit consists of a UTC-PD and a short-stub circuit containing a coplanar waveguide (CPW) stub and a capacitor. In addition to the device parameters, CPW length, which is also a parameter, determines the resonant frequency, the peak output power, and the bandwidth. The short-stub circuit simultaneously acts as an integrated bias circuit, which eliminates hybrid integration of a fine-structure bias-line in the waveguide-output module. For comparison, a UTC-PD without the bias circuit was also considered in the calculation.

Fig. 2 compares the calculated relative output power against the frequency for the matching-circuit-integrated UTC-PD (solid curve) and a discrete UTC-PD with a 50-Ω load (broken curve). The peak output power and the bandwidth of the matching-circuit-integrated UTC-PD are in a tradeoff relationship [7]. A CPW stub length of 70 μm was chosen as an optimum value that would provide a peak output power at around 120 GHz within a device having capacitance (a sum of junction and parasitic capacitances [7]) and parasitic resistance of 45 fF and 6 Ω, respectively. Here, the intrinsic carrier-traveling-time limited bandwidth was assumed to be 120 GHz, and the effective load resistance ($R_{\rm L}$) was designed to be 50 Ω at 120 GHz. Such a moderately large load resistance value gave an increased output power with a relatively wide bandwidth [7]. The output power rolloff relationship with increasing frequency in the discrete UTC-PD shown in Fig. 2 is mainly due to the CR time constant. In contrast, the relative response of the matching-circuit-integrated device has a peak and is about three times higher than that of the discrete UTC-PD at 120 GHz due to the much lower influence of the junction capacitance. This is a clear indication that the matching circuit is effective for increasing the O/E conversion efficiency of the PD at designed frequencies.

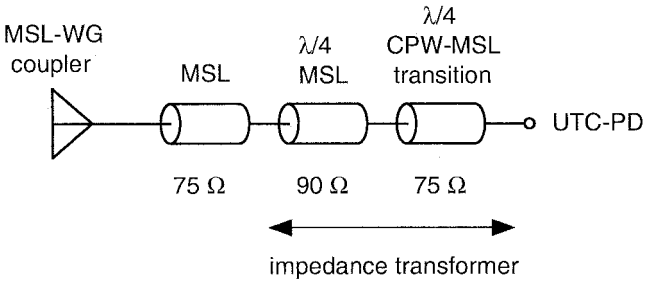

Fig. 3. Circuit diagram of the transformer connecting the UTC-PD and the rectangular waveguide.

The output signal from the PD chip should be electrically connected to the rectangular waveguide output port by means of a low-loss and less frequency-dependent transformer. For this purpose, a microstrip-line (MSL)-based transformer (Fig. 3) was designed and fabricated using a quartz substrate (thickness: 150 μm). It has an impedance transformer on the PD side and an MSL-to-rectangular-WG coupler on the other side. The impedance transformer consists of two quarter-wavelength ($\lambda/4$) WGs was employed to connect the 50-Ω CPW on the InP substrate with the 75-Ω MSL on the coupler side. The characteristic impedances of the first and the second $\lambda/4$ WGs were designed to be 75 and 90 Ω. When the transformer is fabricated on quartz (small dielectric constant) substrate, the larger characteristic impedance for the first WG (CPW-to-MSL transition) is preferable because it allows us to make a smooth connection of the electrode pattern to the CPW having the smaller characteristic impedance fabricated on InP (large dielectric constant) substrate. The third MSL (75 Ω) connects the impedance transformer to the MSL-to-WG coupler (rectangular probe). Fig. 4 shows the return loss of the entire circuit in Fig. 3 against the frequency calculated by using a three-dimensional numerical simulator (High Frequency Structure Simulator: HFSS). Here, the size of the coupler and the back-short depth were chosen to be 390 $\times$ 220 μm and 640 μm, respectively, as optimum values. As seen in this figure, the return loss is less than -10 dB in the entire frequency range in the F-band, and the transmittance of this transformer has nearly flat frequency dependence and is larger than -0.5 dB in the F-band. These results indicate that the frequency characteristics of the designed UTC-PD module should be mainly determined by the frequency characteristics of the short-stub matching circuit, and the output power will be effectively transmitted from the UTC-PD to the rectangular WG.

III. Fabrication and Characterization

The UTC-PD epilayers were grown on a (100) oriented semi-insulating InP substrate by low-pressure metal-organic chemical-vapor deposition (MOCVD). The p-type and n-type

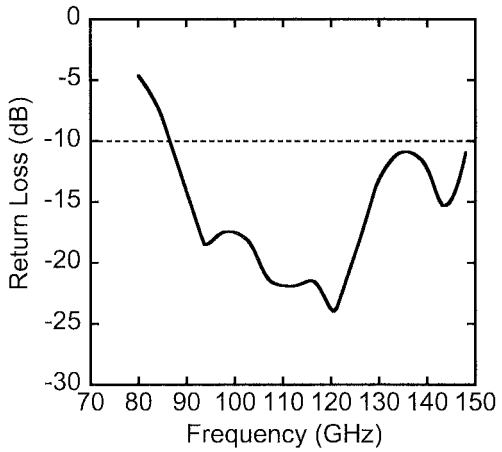

Fig. 4. Calculated return loss of the transformer shown in Fig. 3.

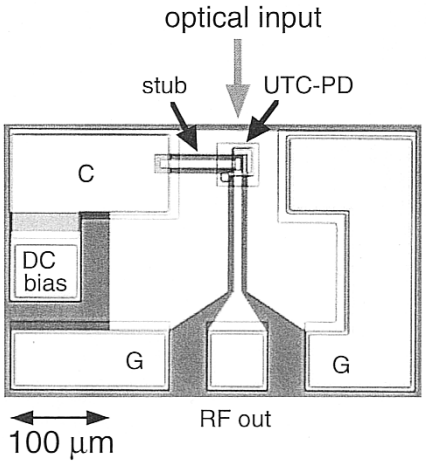

Fig. 5. Micrograph of the fabricated UTC-PD with an integrated matching circuit.

dopants were C and Si, respectively. The absorption layer consists of p-InGaAs ($p = 4 \times 10^{17}/\mathrm{cm}^3$, 122 nm), p-InGaAs ($p = 1 \times 10^{18}/\mathrm{cm}^3$, 10 nm), and undoped InGaAs (8 nm), and the collection layer consists of undoped InGaAsP (16 nm), undoped InP (6 nm), n-InP ($n = 1 \times 10^{18}/\mathrm{cm}^3$, 7 nm), and n-InP ($n = 2 \times 10^{16}/\mathrm{cm}^3$, 201 nm). The rest of the structure is similar to ones reported previously [5], [13]. Hexagonally shaped double-mesa edge-illuminated refracting-facet UTC-PDs with an absorption area (S) of 74 $\mu\mathrm{m}^2$ were fabricated by wet chemical etching and metal-liftoff processes. This relatively large absorption area for increasing the maximum output power is possible because the matching circuit effectively compensates the imaginary part of the internal impedance of the UTC-PD. Each device was integrated with 50-Ω CPWs (one for the output, one for the short-stub) on the InP substrate. These passive elements were monolithically integrated without employing an additional process step in the standard UTC-PD process. The metal–insulator–metal capacitor has a capacitance of 2 pF. Then, the refracting facet structure [14] was fabricated on the side of the PD by using the spontaneous etch-stop nature of InP on the (111)A facet. The side of the device was then antireflection coated and the wafer was cleaved into chips.

A micrograph of the fabricated device is shown in Fig. 5. The chip size is 300×450 μm, and all elements are integrated within this small area. The responsivity measured in a broad-area device at $\lambda = 1.55$ μm was 0.4 A/W. The capacitance and series resistance of the fabricated device were evaluated to be about 45 fF and 6 Ω, respectively, including parasitic elements. The carrier-traveling-time limited bandwidth was characterized to be about 120 GHz in a small area device ($S = 11$ $\mu\mathrm{m}^2$, $R_\mathrm{L} = 25\,\Omega$) using the electrooptic sampling technique [15].

To maintain good fabrication yield and performance reproducibility, the module should be compatible with standard electrical/optical assembly technology. We therefore developed a waveguide output UTC-PD module whose size and configuration are equivalent to those of the conventional butterfly-type O/E device module. Fig. 6 is a schematic drawing of the module configuration, and Fig. 7 is a micrograph of the central part of the module. The transformer connecting the UTC-PD and the WR-8 waveguide was placed in a trench (width $\times$ height $=$ 0.6×0.5 mm) on a submount, and the UTC-PD chip was electrically connected to the quartz transformer using gold ribbons. A dc bias pad was also electrically connected to the dc-bias port on the side of the package through a series resistor (50 Ω) and a parallel capacitor (2.2 nF) to protect the PD from external electrical surges. Then, a fixed back-short, which eliminates mechanical tuning, was placed on the submount. Thus, the output signal goes to the bottom side of the submount shown in Fig. 6. Finally, the photodiode was optically coupled to the optical fiber using a two-lens system, and these optical parts were welded onto the package using an automated YAG laser welder. This assembly technique provides highly stable optical alignment between the photodiode and optical fiber. The entire fabrication sequence is quite similar to that of the conventional O/E device module, so that standard assembly/testing equipment can be used. The optical beam was slightly defocused on the device, so that the effective responsivity became about 0.35 A/W.

Fig. 8 shows a photograph of the fabricated module connected to the WR-8 waveguide. The module size is $12.7 \times 30 \times 10$ mm, excluding the optical fiber. The rectangular waveguide output port is located on the bottom side of the module and connected to a standard F-3922/67B-008 flange using a miniaturized waveguide extension. A miniature SMC connector was used as the dc bias port.

The mm-wave output characteristics of the fabricated modules were measured using a power meter (DORADO, DS-28–6A). For the output power characterization, pulse trains from an actively mode-locked laser diode operating at 60 GHz were optically multiplexed by using an optical multiplexer [16] to prepare quasi-sinusoidal 120-GHz mm-wave light signal ($\lambda = 1.55$ μm, full-width half maximum: 1.5 ps). For the measurement of frequency characteristics, the optical sinusoidal signal was prepared by two-mode beating using two wavelength-tunable laser diodes ($\lambda \approx 1.55$ μm) so that the mm-wave frequency could be changed in a very wide range. The optical modulation index of this signal was close to unity.

IV. Experimental Results

Fig. 9 shows the relationship between measured mm-wave output power and input optical power for the fabricated module

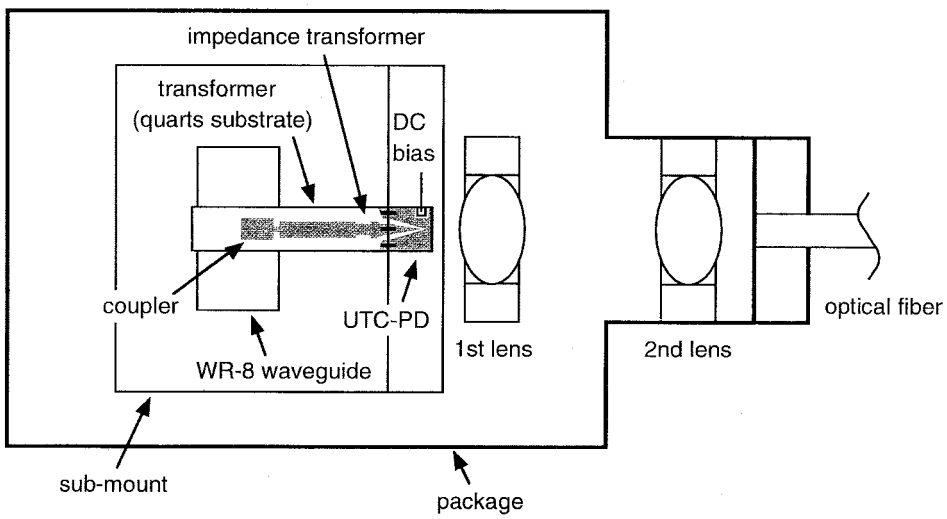

Fig. 6. Schematic drawing of the module configuration.

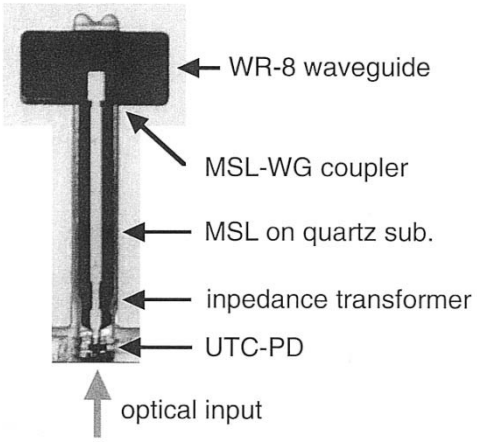

Fig. 7. Micrograph of the transformer connecting the UTC-PD and the rectangular waveguide.

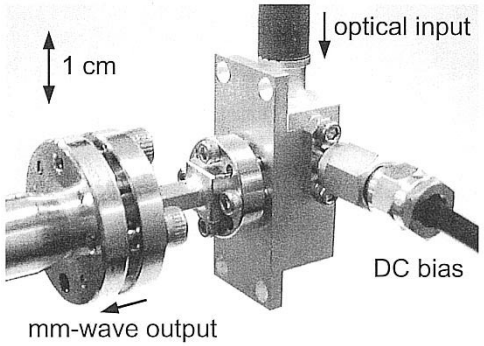

Fig. 8. Photograph of the waveguide-output URC-PD connected to the WR-8 waveguide port.

at a frequency of 120 GHz. The slope is nearly quadratic, indicating that the output power is linearly proportional to the square of the photocurrent. Such a relationship is maintained up to a very high mm-wave output power of over 10 mW. The saturation point of the output power increased with increasing bias

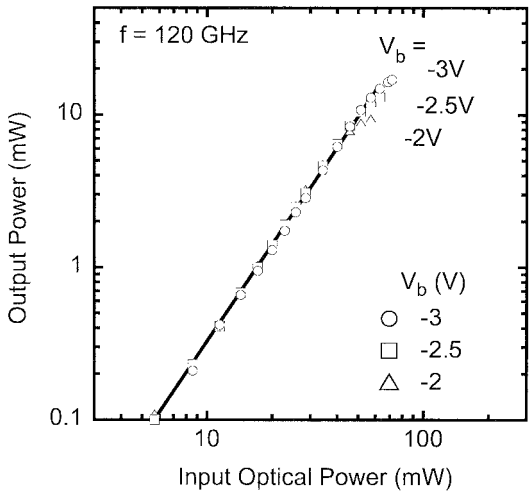

Fig. 9. Relationships between the measured mm-wave output power and input optical power at 120 GHz for several bias voltages.

voltage, and the maximum output power of 17 mW (at a photocurrent of 25 mA), was obtained at a bias voltage of -3 V. To our knowledge, this is the highest mm-wave output power directly generated from a PD module in the F-band. The variation of the maximum output power against bias voltage is attributed to both the shift in the operating voltage along the load line and the space-charge effect in the collection layer [7].

Fig. 10 shows the output power against frequency for a photocurrent of 10 mA. The output 3-dB bandwidth was about 55 GHz, which fully covers the F-band. The solid curve in the figure is a fitting calculation based on an analytical model of the matching circuit. The same parameters assumed in Fig. 2 were used in this fitting, and only relative magnitude was adjusted. The experimental result agrees well with the calculation, indicating that most of the frequency variation is that of the integrated matching circuit, and thus the frequency variation of the transformer is considered to be reasonably flat in the measured range. In addition, the steep decrease of the

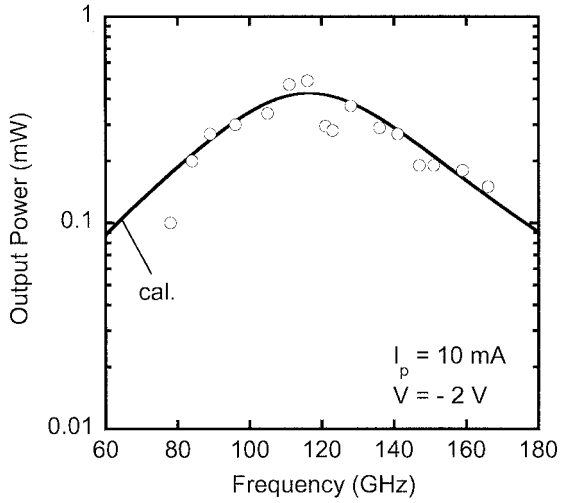

Fig. 10. Output powers from the module against frequency. The solid curve in the figure is a calculation based on an analytical model.

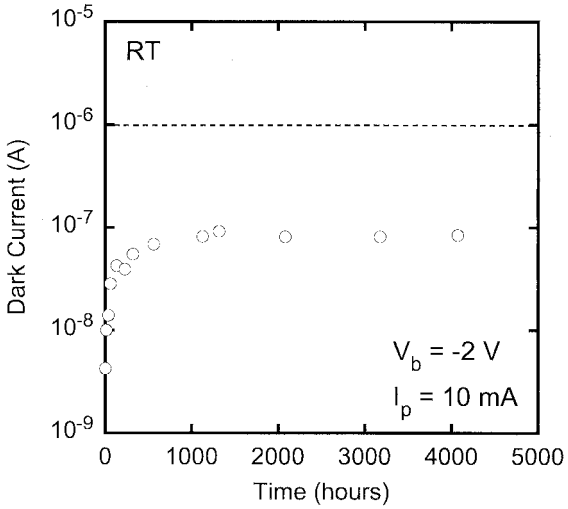

Fig. 12. Variation of the dark current against time under optical input and reverse bias stresses.

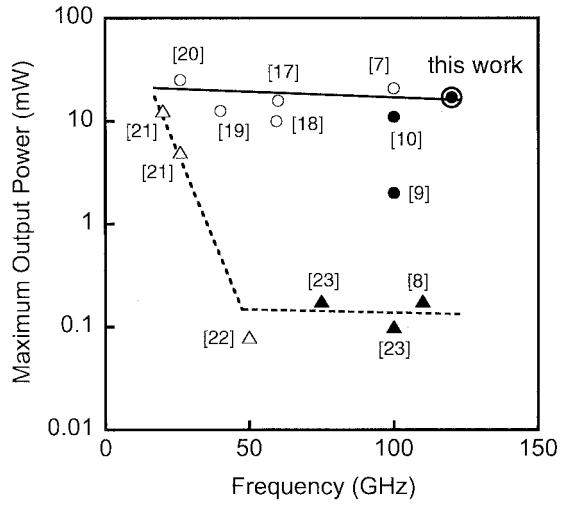

Fig. 11. Comparison of reported mm-wave output power against the operation frequency for UTC-PDs and pin-PDs. Circles are for UTC-PDs and triangles for pin-PDs. Open marks are for chips, and closed ones for modules. Numbers in the figure correspond to the references.

output power at the low-frequency side is due to the cutoff characteristics of the WR-8 waveguide (at 73.8 GHz), which were not included in the calculation. In the high-frequency region, on the other hand, the output power does not decrease steeply with increasing frequency. This is because higher order mode output is possible in the frequency region above 147.6 GHz.

Fig. 11 summarizes the reported maximum RF output powers against the operation frequency for UTC-PDs [9], [10], [17]–[20] and conventional pin-PDs [8], [21]–[23]. The difference between the two types of devices becomes larger as the frequency increases, and the output power of the UTC-PDs becomes about two orders of magnitude larger at around 120 GHz, reflecting their much higher saturation current level. These results clearly demonstrate that the UTC-PD is a promising device for generating high-power mm-wave signals without electrical power amplifiers. Moreover, the output power from the UTC-PD module in this paper is comparable to those obtained by the UTC-PD chips. This implies that the transformer connecting the UTC-PD to the rectangular waveguide has a low transmission loss.

For practical use, long-term stability is also an important issue. Although bias-temperature and optical-input stress tests have confirmed that UTC-PDs designed for 40-Gb/s optical communication systems have excellent reliability [24], we also measured the variation of dark current in the fabricated waveguide-output module under optical input stresses at room temperature (Fig. 12). Here, the module designed for the operation in the W-band [10] was used. The internal configuration of this module is identical to that for the F-band. The module was biased at -2 V with an optical input corresponding to a photocurrent of 10 mA (responsivity is about 0.35 A/W). Except for the initial increase, the dark current stays at a very low level for more than 4000 h. These values are considerably lower than the generally required level for high-speed PDs of 1 μA (broken line in Fig. 12). This indicates that the fabricated UTC-PD chip is reasonably reliable. The changes in responsivity and mm-wave output power at the same photocurrent were also confirmed to be very small after this long-term stability test. These results indicate that the optical alignment by YAG laser welding as well as the device parameters, such as series resistance and junction capacitance, are quite stable.

V. Conclusion

We have designed and fabricated a unitraveling-carrier photodiode module having a rectangular waveguide output port for operation in the F-band. The module is designed to be compatible with the standard assembly technology. It exhibits a record maximum saturation output power of 17 mW at 120 GHz and a 3-dB bandwidth as wide as 55 GHz, which fully covers the F-band. The stability of the module was characterized

under an optical input stress (photocurrent= 10 mA). It was found that the dark current stays at a sufficiently low level for more than 4000 h, and the mm-wave output power does not change during that time. These results clearly demonstrate that the waveguide-output UTC-PD module is highly promising for use as a high-power photonic mm-wave generator in various applications, such as mm-wave wireless communications systems, mm-wave imaging systems, and a photonic local oscillator system in radio telescopes.

ACKNOWLEDGMENT

The authors thank T. Nagatsuma and A. Hirata for their valuable discussions on the measurements, J. Yumoto for his continuous encouragement, and Prof. M. Ishiguro of National Astronomical Observatory of Japan for his stimulating discussions on photonic mm-wave sources.

REFERENCES

[1] A. J. Seeds, "Broadband wireless access using millimeter-wave over fiber systems," in *Tech. Dig. Int. Microwave Symp.*, 1997, pp. 23–25.

[2] T. Nagatsuma, "Progress in instrumentation and measurement toward millimeter-wave photonics," in *Tech. Dig. Int. Topical Meeting Microwave Photonics*, 1999, pp. 91–94.

[3] A. Sasaki and T. Nagatsuma, "Millimeter-wave imaging using an electrooptic detector as a harmonic mixer," *IEEE J. Select. Topics Quantum Electron.*, vol. 6, pp. 735–740, 2000.

[4] J. Payne, B. Shillue, and A. Vaccari, "Photonic techniques for use on the atacama large millimeter array," in *Tech. Dig. Int. Topical Meeting Microwave Photonics*, 1999, pp. 105–108.

[5] T. Ishibashi, N. Shimizu, S. Kodama, H. Ito, T. Nagatsuma, and T. Furuta, "Uni-traveling-carrier photodiodes," *Tech. Dig. Ultrafast Electronics Optoelectronics*, pp. 83–87, 1997.

[6] H. Ito, T. Furuta, S. Kodama, and T. Ishibashi, "InP/InGaAs uni-travelling-carrier photodiode with 310 GHz bandwidth," *Electron. Lett.*, vol. 36, pp. 1809–1810, 2000.

[7] H. Ito, T. Nagatsuma, A. Hirata, T. Minotani, A. Sasaki, Y. Hirota, and T. Ishibashi, "High-power photonic millimeter-wave generation at 100 GHz using matching-circuit-integrated uni-travelling-carrier photodiodes," *Proc. Inst. Elect. Eng. Optoelectron.*, vol. 150, pp. 138–142, 2003.

[8] P. G. Huggard, B. N. Ellison, P. Shen, N. J. Gomes, P. A. Davis, W. P. Shillue, A. Vaccari, and J. M. Payne, "Generation of millimeter and submillimeter waves by photomixing in 1.55 μm wavelength photodiode," *Electron. Lett.*, vol. 38, pp. 327–328, 2002.

[9] T. Noguchi, A. Ueda, H. Iwashita, Y. Sekimoto, M. Ishiguro, T. Ishibashi, H. Ito, and T. Nagatsuma, "A photonic local oscillator for SIS mixer in the 100 GHz band," in *Abstract 13th Int. Symp. Space Terahertz Technology*, vol. 6.1, 2002.

[10] H. Ito, T. Furuta, T. Ito, Y. Muramoto, K. Tsuzuki, K. Yoshino, and T. Ishibashi, "W-band uni-travelling-carrier photodiode module for high-power photonic millimeter-wave generation," *Electron. Lett.*, vol. 38, pp. 1376–1377, 2002.

[11] M. Ishiguro, Y. Sekimoto, A. Ueda, S. Iguchi, T. Noguchi, J. M. Payne, L. R. D'Addario, and W. Shillue, "A hybrid option for the first LO's using direct photonic LO driver," ALMA, Memo 435, 2002.

[12] H. Ito, Y. Hirota, A. Hirata, T. Nagatsuma, and T. Ishibashi, "11 dBm photonic millimeter-wave generation at 100 GHz using uni-travelling-carrier photodiode," *Electron. Lett.*, vol. 37, pp. 1225–1226, 2001.

[13] T. Ishibashi, T. Furuta, H. Fushimi, S. Kodama, H. Ito, T. Nagatsuma, N. Shimizu, and Y. Miyamoto, "InP/InGaAs uni-traveling-carrier photodiodes," *IEICE Trans. Electron.*, vol. E83-C, pp. 938–949, 2000.

[14] H. Fukano, Y. Muramoto, K. Takahata, and Y. Matsuoka, "High-efficiency edge-illuminated uni-traveling-carrier-structure refracting-facet photodiode," *Electron. Lett.*, vol. 35, pp. 1664–1665, 1999.

[15] T. Nagatsuma, M. Yaita, M. Shinagawa, K. Kato, A. Kozen, K. Iwatsuki, and K. Suzuki, "Electro-optic characterization of ultrafast photodetectors using adiabatically compressed soliton pulses," *Electron. Lett.*, vol. 30, pp. 814–816, 1994.

[16] A. Hirata, M. Harada, and T. Nagatsuma, "3-Gb/s wireless data transmission using a millimeter-wave photonic techniques," in *Tech. Dig. 3rd Japan-Korea Joint Workshop Microwave and Millimeter-Wave Photonics*, 2002, pp. 95–98.

[17] T. Nagatsuma, N. Sahri, M. Yaita, T. Ishibashi, N. Shimizu, and K. Sato, "All optoelectronic generation and detection of millimeter-wave signals," in *Tech. Dig. Int. Topical Meeting Microwave Photonics*, 1998, pp. 5–8.

[18] H. Ito, T. Ohno, H. Fushimi, T. Furuta, S. Kodama, and T. Ishibashi, "60 GHz high output power uni-travelling-carrier photodiodes with integrated bias circuit," *Electron. Lett.*, vol. 36, pp. 747–748, 2000.

[19] N. Shimizu, Y. Miyamoto, A. Hirano, K. Sato, and T. Ishibashi, "RF saturation mechanism of InP/InGaAs uni-travelling-carrier photodiode," *Electron. Lett.*, vol. 36, pp. 750–751, 2000.

[20] H. Ito, H. Fushimi, Y. Muramoto, T. Furuta, and T. Ishibashi, "High-power photonic microwave generation at K- and Ka-bands using a uni-traveling-carrier photodiode," *J. Lightwave Technol.*, vol. 20, pp. 1500–1505, 2002.

[21] K. J. Williams, R. D. Esman, and M. Dagenais, "Nonlinearities in p-i-n microwave photodetectors," *J. Lightwave Technol.*, vol. 14, pp. 84–96, 1996.

[22] G. Unterbörsch, D. Trommer, A. Umbach, and G. G. Mekonnen, "High-bandwidth 1.55 μm waveguide integrated photodetector," in *Proc. 8th Int. Conf. Indium Phosphide Related Materials*, 1996, pp. 203–206.

[23] P. G. Huggard, B. N. Ellison, P. Shen, N. J. Gomes, P. A. Davis, W. P. Shillue, A. Vaccari, and J. M. Payne, "Efficient generation of guided millimeter-wave power by photomixing," *IEEE Photon. Technol. Lett.*, vol. 14, pp. 197–199, 2002.

[24] T. Furuta, H. Fushimi, T. Yasui, Y. Muramoto, H. Kamioka, H. Mawatari, H. Fukano, T. Ishibashi, and H. Ito, "Reliability study on uni-traveling-carrier photodiode for a 40 Gbit/s optical transmission systems," *Electron. Lett.*, vol. 38, pp. 332–334, 2002.

Hiroshi Ito (M'92–SM'03) received the B.S. and M.S. degrees in physics and the Ph.D. degree in electrical engineering from Hokkaido University, Japan, in 1980, 1982, and 1987, respectively.

Since joining NTT Laboratories in 1982, he has been involved in research on growth and characterization of III–V compound semiconductors using MBE and MOCVD, and their applications to GaAs- and InP-based heterojunction devices such as bipolar transistors, field-effect transistors, lasers, photodiodes, and integrated optical gates based on electroabsorption modulators. From 1991 to 1992, he was at Stanford University as a Visiting Scientist. His current research involves ultrafast photonic devices for high-bit-rate and millimeter-/submillimeter-wave systems.

Dr. Ito is a Member of the Institute of Electronics, Information and Communication Engineers (IEICE) of Japan, the Japan Society of Applied Physics, and the Physical Society of Japan.

Tsuyoshi Ito (S'97–A'98–M'03) was born in Mie Prefecture, Japan, on September 22, 1973. He received the B.E. and M.E. degrees from Nagoya Institute of Technology, Aichi, Japan, in 1996 and 1998, respectively.

He joined NTT System Electronics Laboratories, Nippon Telegraph and Telephone Corporation, Kanagawa, Japan, in 1998, where he has been engaged in research and development on high-speed optoelectronic devices.

Mr. Ito is a Member of the Japan Society of Applied Physics.

Yoshifumi Muramoto was born in Tokushima, Japan, on March 15, 1967. He received the B.E. and M.E. degrees from Osaka Prefecture University, Osaka, Japan, in 1990 and 1992, respectively.

In 1992, he joined NTT Opto-Electronics Laboratories. He was engaged in research of monolithically integrated photoreceivers and high-speed photodetectors.

Mr. Muramoto is a Member of the Institute of Electronics, Information and Communication Engineers (IEICE) of Japan and the Japan Society of Applied Physics.

Tomofumi Furuta was born in Tokyo, Japan, in 1958. He received the B.S. and M.S. degrees from Tokyo University of Agriculture and Technology, Tokyo, in 1981 and 1983, respectively, and the Ph.D. degree from the University of Tokyo, Tokyo, in 1986, all in electrical engineering.

In 1986, he joined NTT LSI Laboratories, Kanagawa, Japan. He has been engaged in research on semiconductor physics and devices.

Dr. Furuta is a Member of the Japan Society of Applied Physics.

Tadao Ishibashi (M'89–SM'03) was born in Sapporo, Japan, in 1949. He received the Ph.D. degree in applied physics from Hokkaido University, Japan, in 1986.

Since joining NTT Laboratories, Musashino, Tokyo, in 1973, he has been involved in research on semiconductor devices. His work has included submillimeter-wave Si IMPATT diodes, LPE growth of InP/InGaAs materials and their application to field effect transistors, MBE growth of MQW structures, GaAs- and InP-based heterostructure bipolar transistor ICs, ultrahigh-speed photodetectors, and integrated optical switches based on electroabsorption modulators. During 1991 to 1992, he was a Visiting Scientist at Max-Planck-Institute, Stuttgart. He was a Visiting Professor at Tohoku University from 2001 to 2003. In 2001, he joined NTT Electronics, where he is currently working on development of semiconductor optical components for fiber-optic systems.

Dr. Ishibashi received the Ichimura Award in 1992 and the Institute of Electronics, Information and Communication Engineers (IEICE) of Japan Electron Device Society Award in 2002.